Journal of the Serbian Chemical Society
JSCS@tmf.bg.ac.rs • www.shd.org.rs/JSCS
J. Serb. Chem. Soc. 81 (12) S386–S396 (2016) *Supplementary material*

SUPPLEMENTARY MATERIAL TO

Transport properties of binary liquid mixtures – Candidate solvents for optimized flue gas cleaning processes

ANDREJ M. STANIMIROVIĆ[1]*, EMILA M. ŽIVKOVIĆ[2], DIVNA M. MAJSTOROVIĆ[2] and MIRJANA LJ. KIJEVČANIN[2]

[1]*Electric Power Industry of Serbia, Carice Milice 2, 11000 Belgrade, Serbia and* [2]*Faculty of Technology and Metallurgy, University of Belgrade, Karnegijeva 4, 11120 Belgrade, Serbia*

J. Serb. Chem. Soc. 81 (12) (2016) 1427–1439

INDUSTRIAL GASSES EMISSION AND GREENHOUSE EFFECT

The decades-long dynamic development on a global level has resulted in increased consumption of all forms of energy, but also in an increase of greenhouse gas emissions, particularly carbon dioxide, sulphur and nitrogen oxides (CO_2, SO_x and NO_x). Among the largest sources of the mentioned harmful gases are the lignite power plants. The need for environmental protection, as well as increasingly stringent legislation in the field of emissions, requires an increase in the efficiency of the existing process of removing harmful gases from the flue gases of thermal power plants.

Carbon dioxide, originating from fossil fuels, manifests its harmful effect by the appearance of so-called greenhouse effect. The rapid increase in the concentration of carbon dioxide in the atmosphere, and the influence of atmospheric CO_2 on the climate and climate change, prompted the launch of a number of programs of scientific research. The Kyoto Protocol and other international agreements set ambitious targets for reducing the emissions of carbon dioxide and other gases that cause the greenhouse effect. Another serious problem in the field of environmental protection is the acid rains effect. Sulphur oxides (SO_x), among which the most abundant is sulphur dioxide (SO_2), are the main cause of this phenomenon. Like CO_2, sulphur oxides are present in flue gases of thermal power plants and other facilities because of the combustion of fossil fuels containing sulphur.

* Corresponding author. E-mail: andrej_stanimirovic@yahoo.com

TRANSIENT HOT WIRE EXPERIMENTAL SETUP AND MODEL

The underlying model consists of a long thin insulated conductor ("hot wire") surrounded by a large volume of liquid. Thermal conductivity measurement is based on the rate of temperature increase of the hot wire when subjected to a current pulse. Higher thermal conductivity liquid dissipates more heat from the wire, resulting in slower temperature increase and, conversely, less thermally conductive liquid absorbs less heat resulting in faster increase in the hot wire temperature. The best measurement setups have measurement uncertainty of less than 1 %.

When electricity is pulsed through a conductor, it is heated by the Joule effect and part of the generated heat is transferred to the surrounding liquid. The rate of conductor heating is inversely proportional to the intensity of the heat transfer to the surrounding fluid, which in turn depends on the thermal conductivity of the liquid. Thus, knowing the rate of energy flow into the conductor and monitoring the rate of the rise in the conductor temperature, the thermal conductivity of surrounding liquid may be computed. As the temperature of the conductor changes, so does its electrical resistance. The temperature of the conductor is monitored *via* its electrical resistance – analogous to a resistance thermometer and hence, the long thin conductor in these experiments simultaneously played the roles of heat source and temperature sensor.

A long, thin, straight-line conductor generates heat flux per unit length, q, heats itself and by conduction to the surrounding liquid of thermal conductivity k and thermal diffusivity a, at initial temperature T_0. The conductor is assumed to always be at a spatially uniform temperature variable in time.[1,2] The differential equation governing the spatial and temporal temperature change, $T(r,t)$, of the liquid is the Fourier equation in cylindrical coordinates:

$$\frac{1}{a}\frac{\partial T}{\partial t} = \frac{1}{r}\frac{\partial}{\partial r}\left(r\frac{\partial T}{\partial r}\right) \tag{S-1}$$

where $T(r,t) = T_0+\Delta T(r,t)$. The boundary conditions are a constant amount of the heat generated per unit length of the thin conductor and a negligible temperature change far from the conductor. The solution of Eq. (S-1) in the form of an infinite series can after a short time be approximated as:[1]

$$\Delta T = T(r,t) - T_0 = \frac{q}{4\pi k}\left\{-\gamma + \ln\left(\frac{4at}{r^2}\right)\right\} \tag{S-2}$$

where the Euler constant $\gamma = 0.5772$. Differentiating this equation with respect to time for an arbitrary value of radius r yields the following expression:

$$k = \frac{q}{4\pi}\frac{\mathrm{d}\ln(t)}{\mathrm{d}(\Delta T)} \tag{S-3}$$

Thermal conductivity of the liquid, according to this equation, is proportional to the heat flux per unit length of the conductor and inversely proportional to the logarithmic derivative of temperature as a function of time. Equation (S-3) is valid as long as the predominant form of heat transfer is conduction. The occurrence of convection can easily be detected when ΔT, as a function of ln t, deviates from a straight line. Other deviations from the theoretical model have significantly less influence on measurement error.[2]

The uncertainty components calculation started from Eq. (S-3). Since the definition of the temperature coefficient of resistivity can be written in the form $\Delta R = \sigma R_{w0} \Delta T$, it could be rearranged as:

$$k = \sigma R_{w0} \frac{q}{4\pi} \frac{1}{Z_R} \tag{S-4}$$

Therefore, the uncertainty of k depends on the uncertainties of the temperature coefficient of resistivity, σ, the initial value of the hot-wire resistance, R_{w0}, the heat flux per unit length q and the slope of the change of hot-wire resistance *vs*. logarithm of time, *i.e*., $\mathrm{d}\Delta R/\mathrm{d}(\ln t)$ or Z_R. The expanded measurement uncertainty of the setup used in this study was estimated at ±4 %.

Main part of the transient hot wire setup is the hot wire cell. The cell consists of a sample container, a standard test-tube glued to a connecting element, and a hotwire holder, shaped as a hollow half-cylinder that fits into the sample container. The hot wire is completely immersed in the liquid sample in the container.

Hot wire holder is made of copper tubing and standard connecting elements. The relatively high price of the chemicals to be tested in the setup resulted in a requirement that the sample volume be as small as possible. Easy cleaning of the cell and hot wire replacement was another important consideration. Positive tension of the hotwire is provided by a helical spring. The resulting design of the cell provides for quick disassembly, cleaning and reassembly and enables connection to measuring instruments and electrical noise shielding. The cell design can be seen in Fig. S-1.

Chosen hotwire material is chemically stable Alumel alloy of standard composition Ni, 95 %; Al, 2 %; Mn 2 % and Si 1 %. It has a relatively high value of the temperature coefficient of electrical resistance, 23.9×10^{-4} 1/°C. The value for commonly used hotwire material – platinum – is relatively similar, 39.2×10^{-4} 1/°C. Commercially available Alumel conductor TFAL-003-50 by OMEGA® was used in this study. Its overall diameter was 230 μm, 70-μm diameter of the wire and an 80-μm thick Teflon® coating. The coating has good dielectric properties, it is chemically stable, resistant to corrosion and tolerates very low and high temperatures without developing cracks. The length of the hotwire was 132 mm. The inner diameter of the sample reservoir was 16 mm, while the internal

diameter of the hotwire holder, or approximate diameter of the sample, was 13 mm. The sample volume was approximately 27 mL.

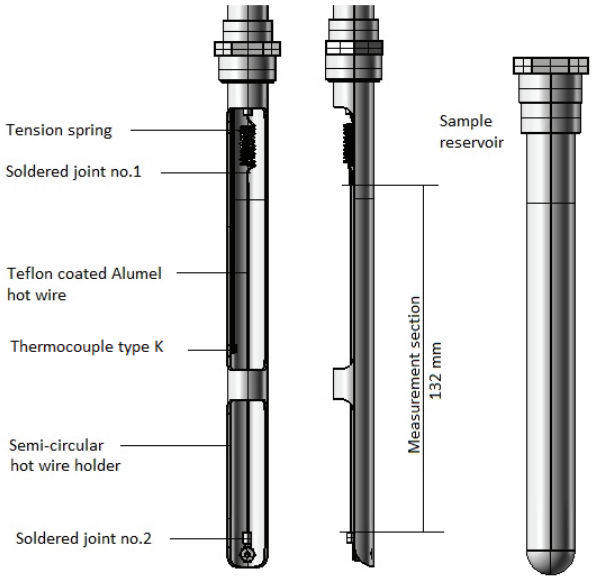

Fig. 1. Hot wire cell.

Sample cell was immersed in a thermostatic water bath, a large 3 L glass beaker equipped with an immersible 600 W heater, a temperature homogenization mixer and digital temperature controller with a K-type thermocouple sensor. The bath temperature is regulated to within ±0.1 °C stability. The sample temperature was monitored by another K-type thermocouple mounted inside the sample cell. The measurement electronics, *i.e.*, a standard series resistor, a current pulse generator and a data acquisition system, was housed in an aluminium box mechanically attached to the hotwire holder.

Current pulse runs through a series connection of the standard resistor and hotwire. The voltage signals across the standard resistor and hotwire were measured by a computer-controlled data acquisition system NI6009 manufactured by National Instruments®. The thermocouple signal was monitored between current pulses to ensure that steady state was re-established before the next pulse was applied. Value of the standard resistor used was 9.60 Ω at room temperature and that of the hotwire was approximately 10 Ω.

For this experimental setup, a program for collection, initial processing and storage of collected data was developed in the LabView® programming environment. The operation of the setup was controlled *via* NI6009 digital outputs. The measurement procedure consisted of 100 heating current pulses repeated at 6 temperatures, between 25 and 50 °C with 5 °C increments. Each pulse lasted for

2 s, after which the temperature field in the sample relaxed for 58 s. Data acquisition conducted during the pulses acquired voltage signals on the standard resistor and hot wire, which yielded temperature and heating power signals for the duration of the pulses. 100 values of the thermal conductivity were calculated from the collected data at each of the 6 steady state temperatures of the sample. A line fitted through the 600 points represents the measured thermal conductivity as a function of temperature.

DENSITY AND VISCOSITY MEASUREMENTS

Measurement is based on the relation between the oscillation period of the U-tube filled with the liquid sample and its density. The cell used for dynamic viscosity measurements contained a straight tube filled with sample, which rotates at a constant speed. A measuring rotor, made of low-density material with a built-in magnet, floats in this tube. An eddy current field is induced by the rotating magnet in the SVM 3000 viscometer with a speed-dependent brake torque. The equilibrium between the viscosity-dependent driving torque, proportional to the speed difference between the tube and the rotor, and the brake torque caused by eddy currents determines the constant speed the rotor will reach shortly after the start of the experiment.

TABULATED EXPERIMENTAL DATA

TABLE S-I. Thermal conductivities λ, deviations $\Delta\lambda$, viscosities η and viscosity deviations $\Delta\eta$ of the investigated binary mixtures; [s]tandard uncertainties u for each variables were $u(T) = \pm 0.01$ K ; $u(p) = \pm 5$ % ; $u(x_1) = \pm 0.0001$, and the combined expanded uncertainties U_c were $U_c(\lambda) = \pm 4.0$ %; $U_c(\eta) = \pm 1.0$ %; at the 0.95 level of confidence ($k \approx 2$)

x_1	λ / W m^{-1} K^{-1}	$\Delta\lambda$ / W m^{-1} K^{-1}	η / mPa s	$\Delta\eta$ / mPa s
MEA(1) + TEGDME (2)				
		298.15 K		
0.0000	0.1649	–	3.3316	–
0.2000	0.1736	–0.0053	3.5839	–2.8580
0.4000	0.1836	–0.0093	4.2943	–5.2579
0.6000	0.1895	–0.0175	5.8373	–6.8251
0.8000	0.1994	–0.0216	9.4298	–6.3429
1.0000	0.2349	–	18.883	–
		303.15 K		
0.0000	0.1637	–	2.9650	–
0.2000	0.1723	–0.055	3.1636	–2.1974
0.4000	0.1825	–0.0096	3.7356	–4.0214
0.6000	0.1884	–0.0178	4.9658	–5.1872
0.8000	0.1983	–0.0221	7.7422	–4.8068
1.0000	0.2346	–	14.945	–
		308.15 K		
0.0000	0.1627	–	2.6570	–
0.2000	0.1714	–0.0057	2.8153	–1.7293
0.4000	0.1812	–0.0101	3.2794	–3.1528

TABLE S-I. Continued

x_1	λ / W m^{-1} K^{-1}	$\Delta\lambda$ / W m^{-1} K^{-1}	η / mPa s	$\Delta\eta$ / mPa s
MEA(1) + TEGDME (2)				
308.15 K				
0.6000	0.1870	–0.0187	4.2697	–4.0501
0.8000	0.1972	–0.0226	6.4989	–3.7085
1.0000	0.2343	–	12.095	–
313.15 K				
0.0000	0.1617	–	2.4004	–
0.2000	0.1704	–0.0058	2.5233	–1.3681
0.4000	0.1801	–0.0104	2.8889	–2.4934
0.6000	0.1857	–0.0194	3.6801	–3.1932
0.8000	0.1962	–0.0232	5.4547	–2.9095
1.0000	0.2339	–	9.8552	–
318.15 K				
0.0000	0.1606	–	2.1791	–
0.2000	0.1693	–0.0059	2.2786	–1.1085
0.4000	0.1790	–0.0109	2.5890	–2.0061
0.6000	0.1847	–0.0198	3.2522	–2.5509
0.8000	0.1953	–0.0237	4.7004	–2.3107
1.0000	0.2336	–	8.2191	–
323.15 K				
0.0000	0.1596	–	1.9902	–
0.2000	0.1682	–0.0061	2.0878	–0.8833
0.4000	0.1777	–0.0114	2.3461	–1.6059
0.6000	0.1833	–0.0204	2.9029	–2.0299
0.8000	0.1943	–0.0242	4.0929	–1.8208
1.0000	0.2332	–	6.8946	–
MEA (1) + PEG 200 (2)				
298.15 K				
0.0000	0.2021	–	51.872	–
0.2001	0.1880	–0.0206	55.320	10.049
0.4001	0.1893	–0.0259	57.425	18.752
0.6000	0.1922	–0.0296	54.650	22.571
0.8000	0.1990	–0.0293	41.403	15.922
1.0000	0.2349	–	18.883	–
303.15 K				
0.0000	0.2017	–	40.557	–
0.2001	0.1875	–0.0208	42.894	7.4620
0.4001	0.1888	–0.0261	44.137	13.827
0.6000	0.1916	–0.0298	41.744	16.554
0.8000	0.1985	–0.0295	31.824	11.757
1.0000	0.2346	–	14.945	–
308.15 K				
0.0000	0.2014	–	32.284	–
0.2001	0.1870	–0.0210	33.885	5.6408
0.4001	0.1883	–0.0262	34.581	10.375
0.6000	0.1908	–0.0303	32.525	12.354
0.8000	0.1980	–0.0297	24.925	8.7922
1.0000	0.2343	–	12.095	–

TABLE S-I. Continued

x_1	λ / W m^{-1} K^{-1}	$\Delta\lambda$ / W m^{-1} K^{-1}	η / mPa s	$\Delta\eta$ / mPa s
MEA (1) + PEG 200 (2)				
313.15 K				
0.0000	0.2010	–	26.045	–
0.2001	0.1862	–0.0214	27.147	4.3416
0.4001	0.1875	–0.0267	27.496	7.9285
0.6000	0.1903	–0.0304	25.715	9.3839
0.8000	0.1974	–0.0299	19.786	6.6928
1.0000	0.2339	–	9.8552	–
318.15 K				
0.0000	0.2007	–	21.429	–
0.2001	0.1856	–0.0216	22.182	3.3963
0.4001	0.1870	–0.0269	22.307	6.1633
0.6000	0.1898	–0.0306	20.760	7.2569
0.8000	0.1969	–0.0301	16.055	5.1939
1.0000	0.2336	–	8.2191	–
323.15 K				
0.0000	0.2003	–	17.922	–
0.2001	0.1851	–0.0218	18.424	2.7086
0.4001	0.1864	–0.0271	18.400	4.8901
0.6000	0.1892	–0.0308	17.045	5.7394
0.8000	0.1964	–0.0302	13.239	4.1389
1.0000	0.2332	–	6.8946	–

Table S-II. Parameters of Redlich–Kister correlation and the corresponding RMSD for thermal conductivity deviation, $\sigma(\Delta\lambda)$ / W m^{-1} K^{-1}, and viscosity deviations, $\sigma(\Delta\eta)$ / mPa s, of the investigated binary mixtures

Function	T / K	A_0	A_1	A_2	σ
MEA (1) + TEGDME (2)					
$\Delta\lambda$	298.15	–0.0523	–0.0850	–0.0879	0.00002
	303.15	–0.0533	–0.0862	–0.0914	0.00004
	308.15	–0.0563	–0.0888	–0.0902	0.00004
	313.15	–0.0585	–0.0912	–0.0891	0.00010
	318.15	–0.0599	–0.0927	–0.0901	0.00002
	323.15	–0.0627	–0.0942	–0.0885	0.00002
$\Delta\eta$	298.15	–24.318	–18.149	–12.317	0.0872
	303.15	–18.569	–13.588	–9.2141	0.0646
	308.15	–14.543	–10.308	–6.8071	0.0460
	313.15	–11.822	–8.0272	–4.2941	0.0353
	318.15	–9.3238	–6.2606	–3.7805	0.0201
	323.15	–7.4475	–4.8825	–2.7852	0.0160
MEA (1) + PEG 200 (2)					
$\Delta\lambda$	298.15	–0.1106	–0.0440	–0.1259	0.0004
	303.15	–0.1114	–0.0440	–0.1272	0.0006
	308.15	–0.1126	–0.0448	–0.1272	0.0008
	313.15	–0.1137	–0.0431	–0.1292	0.0007
	318.15	–0.1146	–0.0431	–0.1305	0.0009

TABLE S-II. Continued

Function	T / K	A_0	A_1	A_2	σ
		MEA (1) + PEG 200 (2)			
	323.15	–0.1153	–0.0431	–0.1318	0.0016
$\Delta\eta$	298.15	84.641	30.622	–9.7250	0.4403
	303.15	65.047	22.396	–13.892	0.2892
	308.15	48.558	16.436	–9.6139	0.2000
	313.15	36.669	12.268	–6.0824	0.1161
	318.15	27.641	9.3751	–2.2290	0.0973
	323.15	22.549	7.4573	–3.2107	0.0669

DETAILS OF THE EMPLOYED MODELS

For correlating thermal conductivity of mixtures, Filippov[3] suggested a simple correlation:

$$\lambda_m = w_1\lambda_1 + w_2\lambda_2 - 0.72 w_1 w_2 (\lambda_2 - \lambda_1) \quad \text{(S-5)}$$

where w_1 and w_2 are the weight fractions of the components and λ_1 and λ_2 are the thermal conductivities of the components ($\lambda_2 \geq \lambda_1$). The constant 0.72 could be replaced by the parameter determined from the experimental data.

According to method suggested by Jamieson,[4] the thermal conductivity of liquid mixtures is calculated from the equation:

$$\lambda_m = w_1\lambda_1 + w_2\lambda_2 - \alpha(\lambda_2 - \lambda_1)\left[1 - w_2^{0.5}\right] w_2 \quad \text{(S-6)}$$

in which α is an adjustable parameter obtained by data regression.

Baroncini[5] extended the Latini[6] method to binary mixtures:

$$\lambda_m = \left[x_1^2 A_1 + x_2^2 + 2.2\left(\frac{A_1^3}{A_2}\right)^{0.5} x_1 x_2 \right] \frac{(1 - T_{rm})^{0.38}}{T_{rm}^{1/6}} \quad \text{(S-7)}$$

where x_1 and x_2 are the mole fractions, and A_1 and A_2 are model parameters of the components ($A_2 \geq A_1$) calculated from the equation:

$$A = \frac{A^* T_b^{\alpha}}{M^{\beta} T_c^{\gamma}} \quad \text{(S-8)}$$

in which T_b represents the normal boiling point (K), M is the molecular weight (g mol^{-1}) and the parameters A^*, α, β and γ for various organic compounds are available in the literature.[6] The constant 2.2 in Eq. (S-7) could be replaced by an adjustable parameter determined by data regression. The reduced temperature of the mixture, T_{rm} is calculated as:

$$T_{rm} = T / T_{cm} \quad \text{(S-9)}$$

where the critical temperature of the mixture, T_{cm} can be determined from the equation:

$$T_{cm} = x_1 T_{c1} + x_2 T_{c2} \tag{S-10}$$

Rowley[7] model for binary mixtures is based on the equation:

$$\lambda_m = w_1\lambda_1 + w_2\lambda_2 + w_1 w_2 \left[\frac{G_{21}(\lambda_{12} - \lambda_1)}{w_1 + w_2 G_{21}} + \frac{G_{12}(\lambda_{12} - \lambda_2)}{w_2 + w_1 G_{12}} \right] \tag{S-11}$$

where G_{12} and G_{21} are the same NRTL parameters as used for calculating the activity coefficients or in the Eyring-NRTL[8] model for correlating viscosity. The parameter λ_{12} can be determined from the equation:

$$\lambda_{12} = \frac{M_1 (w_1^*)^2 \left(w_2^* + w_1^* G_{12}\right)\lambda_1 + M_2 (w_2^*)^2 \left(w_1^* + w_2^* G_{21}\right)\lambda_2}{M_1 (w_1^*)^2 \left(w_2^* + w_1^* G_{12}\right) + M_2 (w_2^*)^2 \left(w_1^* + w_2^* G_{21}\right)} \tag{S-12}$$

where w_1^* and w_2^* can be calculated as:

$$w_1^* = \frac{M_1 G_{21}^{0.5}}{M_1 G_{21}^{0.5} + M_2 G_{12}^{0.5}} \tag{S-13}$$

$$w_2^* = 1 - w_1^* \tag{S-14}$$

The model parameters were obtained using the Marquardt optimisation technique[9] for the minimization of the objective function defined by the equation:

$$OF = \frac{1}{m} \sum_{i=1}^{m} \left(\frac{Y_{exp} - Y_{cal}}{Y_{exp}} \right)_i^2 \rightarrow \min \tag{S-15}$$

where Y_{exp} and Y_{cal} represent the experimental and calculated values of the thermal conductivity or viscosity and m is the number of experimental data points.

The viscosities of the investigated binary mixtures were correlated by the two-parameter Eyring-NRTL[8] and Eyring-UNIQUAC[10] models, and by the two- and three-parameter McAlister[11] models.

The Eyring-NRTL[8] model is based on the Eyring theory of absolute reaction rates. For a binary mixture, the model is defined by the equation:

$$\ln(\eta_m V_m) = x_1 \ln(\eta_1 V_1) + x_2 \ln(\eta_2 V_2) + \\ + x_1 x_2 \left[\frac{\tau_{21} \exp(-\alpha\tau_{21})}{x_1 + x_2 \exp(-\alpha\tau_{21})} + \frac{\tau_{12} \exp(-\alpha\tau_{12})}{x_2 + x_1 \exp(-\alpha\tau_{12})} \right] \tag{S-16}$$

in which η_m, η_1 and η_2 are the dynamic viscosity of mixture and components 1 and 2, respectively; V_m, V_1 and V_2 are the molar volumes of the mixture and the pure components; x_1 and x_2 are the mole fractions of the components; α, τ_{12} and τ_{21} are model parameters.

Parameter α is a measure of the system non-ideality and is usually set to a constant value (α=0 for ideal mixtures). In this investigation, its value was set to α = 0.3. The parameters τ_{ij} (i = 1,2; j = 2,1) are defined as:

$$\tau_{ij} = \frac{G_{ij} - G_{ji}}{RT} = \frac{\Delta G_{ij}}{RT} \tag{S-17}$$

where G_{ij} and G_{ji} are binary interaction parameters obtained by data regression.

The Eyring-UNIQUAC[10] model is also based on the Eyring theory of absolute reaction rates. Dynamic viscosity of the mixture η_m is calculated from the following equation:

$$\ln(\eta_m V_m) = x_1 \ln(\eta_1 V_1) + x_2 \ln(\eta_2 V_2) + \frac{\Delta^* g^{EC}}{RT} + \frac{\Delta^* g^{ER}}{RT} \tag{S-18}$$

where $\Delta^* g^{EC}$ and $\Delta^* g^{ER}$ are the combinatorial and residual contributions to the excess Gibbs free energy, calculated from the UNIQUAC model, while the other symbols have the same meaning as in Eq. (S-17). The combinatorial part is calculated from the contributions of the functional groups constituting the molecules of the components. Residual part depends on the interactions of the functional groups within the mixture and includes two interaction parameters obtained by data regression. Detailed calculation procedure is described in the literature.[10]

The two-parameter McAllister model (McAllister-3)[11] is defined by the equation:

$$\begin{aligned} \ln \upsilon = {} & x_1^3 \ln \upsilon_1 + 3x_1^2 x_2 \ln \upsilon_{12} + 3x_1 x_2^2 \ln \upsilon_{21} + x_2^3 \ln \upsilon_2 - \\ & - \ln(x_1 + x_2 M_2 / M_1) + 3x_1^2 x_2 \ln[(2 + M_2 / M_1)/3] + \\ & + 3x_1 x_2^2 \ln[(1 + 2M_2 / M_1)/3)] + x_2^3 \ln(M_2 / M_1) \end{aligned} \tag{S-19}$$

where υ_{12} and υ_{21} are the interaction parameters obtained by data regression, and x_i, M_i and υ_i are the mole fraction, molar mass and kinematic viscosity of the pure component i.

Three-parameter McAlister model (McAllister-4)[11] has the form:

$$\begin{aligned} \ln \upsilon = {} & x_1^4 \ln \upsilon_1 + 4x_1^3 x_2 \ln \upsilon_{1112} + 6x_1^2 x_2^2 \ln \upsilon_{1122} + 4x_1 x_2^3 \ln \upsilon_{2221} + \\ & + x_2^4 \ln \upsilon_2 - \ln(x_1 + x_2 M_2 / M_1) + 4x_1^3 x_2 \ln[(3 + M_2 / M_1)/4] + \\ & + 6x_1^2 x_2^2 \ln[(1 + M_2 / M_1)/2] + 4x_1 x_2^3 \ln[(1 + 3M_2 / M_1)/4)] + \\ & + x_2^4 \ln(M_2 / M_1) \end{aligned} \tag{S-20}$$

where υ_{1112}, υ_{1122} and υ_{2221} are adjustable interaction parameters and x_i, M_i and υ_i are the mole fraction, molar mass and kinematic viscosity of the pure component *i*.

The model parameters were determined from Eq. (S-15) using the Marquardt optimization technique.[9]

REFERENCES

1. H. S. Carslow, J. C. Jaeger, *Conduction of Heat in Solids*, Oxford University Press, Oxford, 1959
2. M. Kostic, K. C. Simham, in Proceedings of 6th WSEAS International Conference on Heat and Mass Transfer, Ningbo, China, 2009, p. 71
3. B. E. Poling, J. M. Prausnitz, J. P. O'Connell, *The Properties of Gasses and Liquids*, 5th ed., McGraw–Hill, New York, USA, 2001
4. D. T. Jamieson, J. B. Irving, J. S. Tudhope, *Liquid Thermal Conductivity. A Data Survey to 1973*, H. M. Stationary Office, Edinburgh, UK, 1975
5. C. Baroncini, P. DiFilippo, G. Latini, M. Pacetti, *Thermal Conductivity*, 17th ed., Plenum Pub., New York, USA, 1983
6. G. Latini, M. Pacetti, *Therm. Conduct.* **15** (1977) 245
7. R. L. Rowley, *Chem. Eng. Sci.* **43** (1988) 361
8. L. T. Novak, *Ind. Eng. Chem. Res.* **43** (2004) 2602
9. D. W. Marquardt, *J. Ind. Soc. Appl. Math.* **2** (1963) 431
10. R. J. Martins, M. J. E. D. Cardoso, O. E. Barcia, *Ind. Eng. Chem. Res.* **39** (2000) 849
11. R. A. McAllister, *AIChE J.* **6** (1960) 427.